

Mars 2020 maxon Commercial Motor Development from Commercial-Off-the-Shelf to Flight-Qualified Motors, Gearboxes, and Detent Brakes: Overcoming Issues and Lessons Learned

Michael LoSchiavo*, Robin Phillips**, Rebecca Mikhaylov* and Lynn Braunschweig**

Abstract

Building on previous collaborations, maxon and the Jet Propulsion Laboratory (JPL) established a partnership to modify Ø20-mm & Ø32-mm Commercial-Off-The-Shelf (COTS) BrushLess Direct Current (BLDC) flat motors and a Ø22-mm planetary gearbox. The commercial design was modified to meet the requirements for the Mars 2020 rover, a Class B [1] interplanetary mission operating in the Martian surface environment, while maintaining as much of the industrial heritage as possible. Numerous issues encountered during development were successfully addressed, and qualification of the design and acceptance testing for the 10 Flight Model (FM) actuators installed on the Mars 2020 rover was completed on time for the rover assembly schedule.

Mars 2020 Overview and Previous Missions

maxon brushed motors have significant flight heritage on JPL Mars missions. The Mars Pathfinder Sojourner rover contained 11 brushed direct current (DC) motors based on the RE16 design [2]. The Mars Exploration Rovers (MER), Spirit and Opportunity, each utilized 39 maxon brushed DC motors, based on modified commercial “RE” series designs. At the end of the Opportunity rover’s mission, all of the drive wheel motors were still functioning, having survived 5111 Sols (Martian day/night thermal cycles), with each motor completing $\sim 9 \times 10^7$ revolutions. Spare MER motors (4x RE20 and 5x RE25) were also used as part of the Phoenix lander. maxon has continued to develop brushed motors for the Martian applications Interior Exploration using Seismic Investigations, Geodesy and Heat Transport (InSight) mission and ExoMars mission by modifying newer commercial designs, however, these designs were not viable options for Mars 2020 due to the brush sensitivity to a pyroshock environment.

Mars 2020 is the first step in a potential multimission approach to a Mars Sample Return mission and future human exploration of Mars [3,4]. The primary objective of the Mars Science Laboratory (MSL) and its Curiosity rover is to search for habitability. Mars 2020 [5] and its Perseverance rover will seek signs of past life and collect Martian cores for possible later collection and return to Earth. The Mars 2020 project maximized the use of build-to-print hardware to reduce development risk and much of the project utilizes a large amount of spare MSL hardware (specifically the cruise and descent stages). Mars 2020 also levied design constraints to remain within the MSL footprint in terms of mass, volume, and power on major components, such as the rover chassis, which houses the Sample Caching System (SCS), and large robotic arm.

The SCS is one of the most advanced robotic systems ever developed for planetary exploration, pushing more robotic Degrees of Freedom (DOFs) into a smaller volume than has previously been achieved. Within the SCS, the Adaptive Caching Assembly (ACA) and Coring Drill [6,7,8,9,10] requires complex mechanisms that need gearmotors smaller in volume than any equivalent hardware developed for MSL. Additionally, solenoid brake channels in the motor controller were traded for additional sensor channels, which required any new motors to utilize a passive holding torque mechanism. Tasked with Mars 2020’s mission objective to drill, capture, and store core samples along with volume constraints from the MSL

*Jet Propulsion Laboratory, California Institute of Technology, Pasadena, CA

** maxon international ag, Sachseln, Switzerland

rover, the project required new actuators that then needed to be baselined from proven/existing technologies to meet the launch schedule.

The Curiosity rover had major actuator development issues, which contributed to the launch slipping from 2009 to 2011. The development of several new motors was highlighted as a major reason for the actuator schedule slips [4,11]. The JPL Mars 2020 actuator team considered the lessons learned from the earlier rover mission and decided to leverage an existing COTS design to reduce the flight hardware schedule risk.

maxon has an extensive catalog of motors for industrial use and has proven flight heritage from the MER mission that, with suitable modifications, the motor designs are robust for space applications. maxon COTS flat motors were utilized in the SCS testbeds and baselined in the original derivation of the system volume and functional requirements. A close collaboration between maxon and JPL was essential in developing an up-screened COTS-to-robust, flight flat motor mounted on a \$2B mission. Two motor types, referred to here as M20 and M32 (with 20 and 32 being the COTS motor diameter in millimeters), were based on existing maxon COTS products and chosen to meet the project envelope constraints (Figure 1). The M20 gearmotor includes an integrated gearbox (Figure 1). Additionally, a detent module was added to the M32 to provide a passive holding torque to a static motor. When the motor is spinning above a minimum speed, the inertia is sufficient to overcome any subtractive/additive torques from each detent step, with no significant performance reduction from the motor.

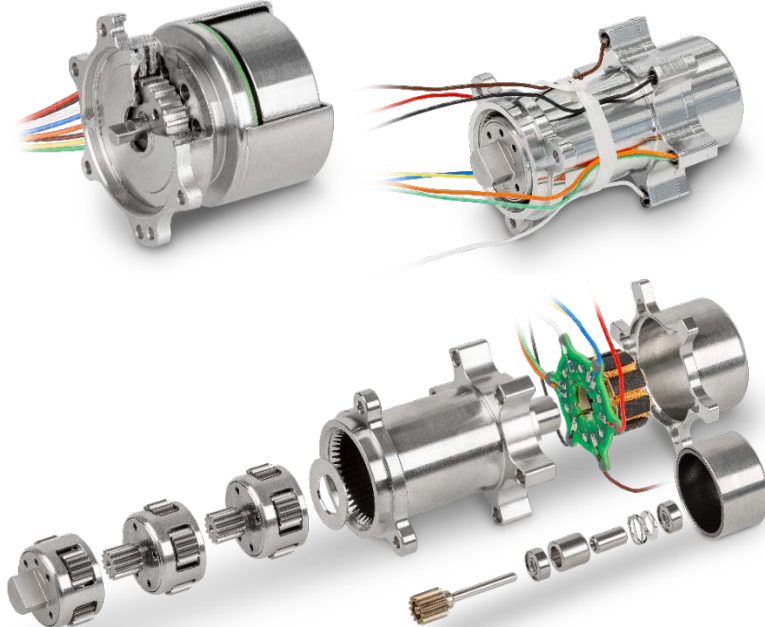


Figure 1. Top Left: M32 motor cut-away showing detent brake; Top Right: M20 FM gearmotor; Bottom: Exploded view of M20 gearmotor

Mars 2020 Mechanism Descriptions

The SCS includes a rotary percussive drill located on the turret at the end of the large robotic arm and the sample tube processing plant internal to the rover (the ACA, Figure 2). A 3-DOF arm in the processing plant passes the tubes and samples to multiple science stations and hermetically seals the tubes. Additionally, a bit carousel passes tubes and bits between the internal ACA and the external drill. Several of the mechanisms in the SCS subsystem are driven using the M32 detent motors described in this paper, which are mated to three different torque amplifying planetary gearboxes to provide a family of actuators (named

SHACD, SAS, and Chuck), designed and manufactured by Sierra Nevada Corporation in Durham, NC. The motors provide the active driving torque and holding torque for the following applications: the 3-DOF Sample Handling Assembly (SHA), which consists of a linear stage and two rotary (shoulder/elbow) joints; the tube gripper and sealing ram within the tube sealing station of the ACA; the central rotating axis of the bit carousel; the mechanism that shifts the coring drill between high-speed drilling and high-torque core break-off modes; and the opening and closing of the chuck at the end of the drill. All of these mechanisms are single-string devices performing a serial task in the sequence of capturing a rock core sample.

The M20 gearmotor utilized similar modifications as developed in the M32 design effort into the smaller motor diameter for the most volume constrained component of the ACA, the end effector. This component is mounted to the end of the SHA and physically grabs the sample tube for transport within the ACA.

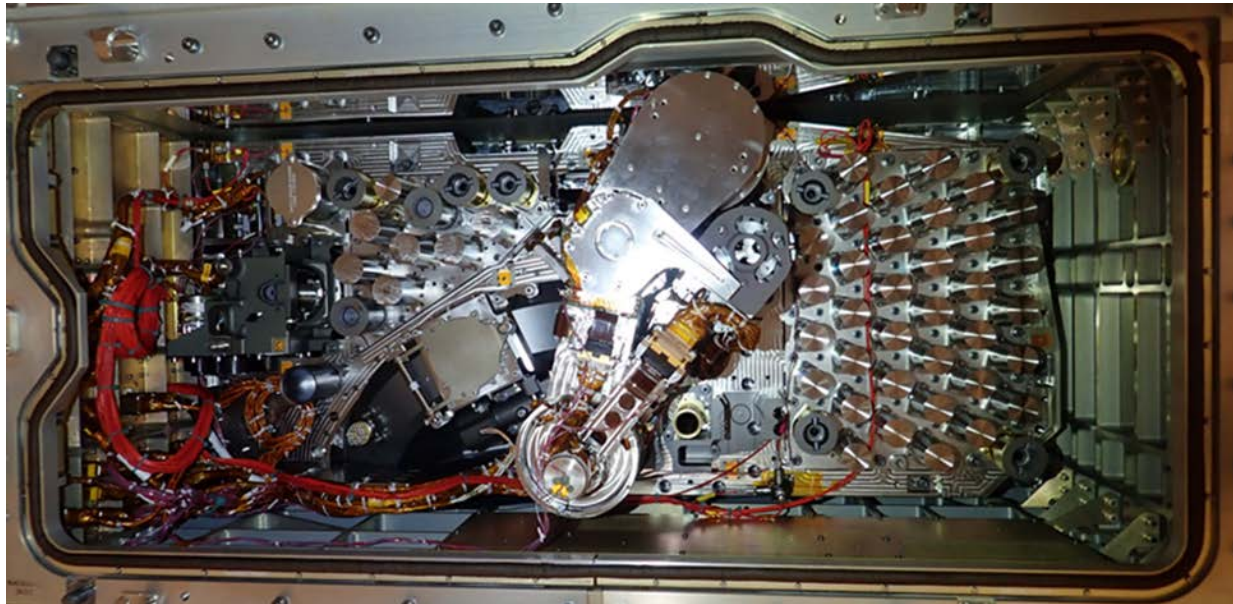


Figure 2. The Adaptive Caching Assembly (ACA)

The end effector has some of the strictest planetary protection and handling requirements ever levied on a mechanism. The Mars Helicopter technology demonstrator mounts to the underbelly of the rover in its stowed configuration and has a one-time actuation of the deployment arm. A summary of the four new designs utilizing the M20 and M32 motors for 10 flight locations on the rover are listed in Table 1.

Table 1. Gearmotor assignments

Application	Gearmotor Name	Motor
SHA Elbow	SHACD	M32
SHA Linear	SHACD	M32
SHA Shoulder	SHACD	M32
Bit Carousel	SHACD	M32
Tube Drop-off	SHACD	M32
Sealing Station	SAS	M32
Core-Break Lock Out	SAS	M32
Helicopter Deployment Arm	SAS	M32
Chuck	Chuck	M32
End Effector	DEE (M20)	M20

Mars 2020 Specific Requirements

There are several key and driving requirements derived from the Mars environment and mission requirements:

1. The mission objective to look for compounds that provide evidence of life on Mars levied strict Contamination Control and Planetary Protection handling, design, and assembly constraints, including: reducing organic materials used for assembly and treating them to minimize outgassing and deposition on crucial components, cleaning all surfaces to prevent contamination from migrating due to handling, and eliminating/reducing viable compounds from spores and organic materials from Earth.
2. The actuators located on the extremities of the rover arm are subjected to wide diurnal temperature changes, which is highly stressing on electronic components and bonded materials.
3. In addition to pyrotechnic release devices, the rotary percussive drill generates an environment that can be defined as a combination of a random vibration, sine vibration, and pyroshock. This environment varies depending on several factors, including the hardness of the rock being drilled into, the percussion frequency used for drilling, and the weight-on-bit applied. Ref. [7] contains more information on the coring drill. The dynamic environment fatigues components and can amplify natural modes in hardware, which then couples with fatigue induced from extreme thermal cycling.

maxon Catalog Flat Motor and Gearbox Design

maxon has 50 years of experience designing and manufacturing brushed and brushless DC electric motors, gearboxes (both planetary and spur), feedback devices, and control electronics. The brushless DC motors are offered in several families of types, covering both ironless winding and iron-core winding types. The iron-core winding types are in turn divided into external and internal rotor families where the rotor mounted permanent magnets are respectively outside or inside the windings. Both the M20 and M32 motors are derived from maxon's "flat motor" family (Figure 3), which are of the BLDC external rotor type.

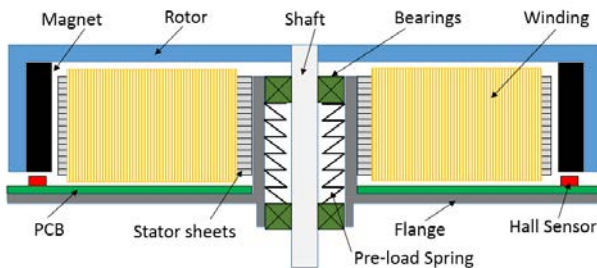


Figure 3. maxon flat motor standard features

For industrial applications, compared to other BLDC types, the flat motors represent a simple, low-cost design that delivers high torque in a short (but large diameter) envelope. When operated without a housing in Earth atmosphere conditions, the exposed spinning outer rotor also enables excellent convective cooling and hence high continuous power ratings.

maxon's flat motor family covers various diameters (14, 20, 32, 45, 60, and 90 mm), all of which share the same basic design. A large-diameter rotor provides the structural support and acts as a magnet return for a ring magnet. This rotor is supported by two ball bearings housed in a flange/bearing support structure. The bearings are preloaded by use of a spring. A stator sheet stack is wrapped with magnet wire and mounted to the bearing support structure while being electrically connected to a printed circuit board (PCB), which also holds three Hall sensors that detect the main magnet position.

maxon has the industrial heritage for the flat motor design, which has been built several million times, including over 1 million units for commercial truck exhaust gas cleaning systems, an application that provides real world proof of the robustness of the basic design.

Flight Fidelity Modifications to the Catalog Designs

It was known from previous maxon work that commercial motor designs usually require some modifications to allow reliable operation in a Martian environment, in particular, the wide temperature range cycling,

vibration/shock environment, and vacuum exposure. After determining that the Ø20 mm and Ø32 mm models provided the optimal power versus mass compromise, the commercial design was analyzed by a team incorporating both JPL and maxon personnel with the intention of applying the previous experience of both organizations to optimize the design for ultimate reliability in the harsh Martian environment. Table 2 lists the features in the COTS design that needed modification.

Table 2. COTS design and modifications for Martian environment

COTS Design	Design Risk for Mars 2020 Application	Solution
Flange bearing carrier out of several parts with dissimilar materials	Connection under shock/vibration; corrosion; coefficient of thermal expansion mismatch	Create one-piece flange/bearing carrier
Standard Hall sensors	Temperature range limitations, failure due to radiation exposure	Use Hall sensor that can be qualified for environmental conditions
Rotor shaft glued to bearing races	Shock and temperature environment breaks adhesive bond and causes rotor to move	Add securing/spacer rings to design and mount all parts on shaft to hard stop. Weld rotor to shaft
Main magnet only partially covered in adhesive	Bond to rotor is not as strong as it could be and might fail under repeated temperature cycling	Develop new bonding application process to ensure at least 80% coverage
Flex-print PCB	Can flex under vibration environment, which leads to mounted components breaking	Replace with FR4 and flying lead wire connections
Winding taps run directly to PCB	~1 cm lengths of unsupported thin wire susceptible to vibration-induced resonance and breakage	Stake winding taps to stator and strain relief with “expansion loops” next to solder joint

In order for the maxon catalog flat motor to survive the requirements of the Mars 2020 mission, several changes were made. The PCB material was changed from a flex print to FR4, a material commonly used for space missions as it does not significantly outgas, is robust enough to support the Hall sensors in a vibration environment, and fulfills IPC-A-600 Class 3 requirements and testing required by JPL. The bearing preload architecture was modified so that the entire system was pushed to a hard stop meaning the individual parts could not shift during impact or vibrations. A more robust spring was selected with shim ends to better distribute the forces and prevent the shim from breaching the bearing. High-quality industrial bearings were selected from one of maxon’s standard suppliers. Braycote 600EF was chosen as the lubrication with a fill-factor (15–20%) of the free volume of each bearing measured (by mass) and documented.

As has been standard practice for decades in space applications, the PCBs in both the M20 and M32 designs have conformal coating to: 1) protect the PCB from corrosion while in storage on the ground awaiting launch; 2) protect against short circuits from any debris in weightless conditions; and 3) suppress any tin whisker growth. maxon had a good experience working with Speciality Coating Systems in the Czech Republic for Parylene HT application for ExoMars and chose to work with them again for the Mars 2020 motors. The fully populated PCBs, including attached stators with windings were shipped to Speciality Coating Systems, coated, and returned to maxon for integration into the rest of the motor.

Undoubtedly the most difficult component choice to be made when designing a space-rated BLDC motor is the rotor angle detector required for the control electronics to correctly commutate the motor. All of maxon’s BLDC motors use various types of Hall sensors for this purpose. As described in Ref. [12], the solution for ExoMars was a radiation and temperature test program with many different types of compact Hall sensors. Unfortunately, the Infineon TLE4945 sensor that was selected for ExoMars has been discontinued, but maxon had already tested and selected a variant of Honeywell’s bipolar SS41 Hall sensor range for other space applications. JPL organized the purchase of a flight batch of sensors that were subjected to additional screening (pre-conditioning, lead tinning, and thermal cycling as well as lot qualification including Destructive Physical Analysis) to qualify the sensor lot prior to delivery to maxon for population onto the PCBs. These sensors have been shown to operate well outside their published range, although performance deteriorates at the temperature extremes. Satisfactory operation can be achieved

between -100°C and $+200^{\circ}\text{C}$. Radiation testing showed no failures after exposure to γ -radiation (absorbed doses of 300 J/kg for 64h).

maxon's flight heritage from the MER mission does not include gearboxes, however, maxon gained considerable experience during the ExoMars development [13] and qualification program. The program demonstrated that although COTS planetary gearboxes, in particular those developed for high-temperature "downhole" oil and gas industry applications, can be easily modified for space applications, significant lifetime problems arise when switching to vacuum-rated lubricants such as Braycote 601EF. ExoMars development work had shown that using a slurry of grease and oil as previously described for Harmonic Drive applications [14] partially mitigated this lubricant issue. The root cause of the lifetime issues is that Braycote 601EF is fundamentally unsuitable for lubricating sliding (as opposed to rolling) surfaces. In order to achieve the lifetime requirements for the ExoMars drill drive, the COTS design sliding motion between each planetary gear and its shaft/axis was converted to rolling motion by the addition of needle bearings, which was then used as the basis for the Mars 2020 gearbox (Figure 4).



Figure 4. Exploded view of M20 planetary gearbox stage

Given the mission-critical nature of the M20 application, the JPL and maxon review teams decided that excessive residual risk remained in connections between sun gears and planetary carriers as well as between the planet axes pins and the carriers. In the COTS design, these connections are press fitted and welded, however, due to the hardened nature of the materials used for the axes and sun gears, the welds always exhibited surface cracks. This is an accepted compromise for industrial applications (and is not known to have ever caused a field failure), but due to the extreme Martian diurnal temperature cycling, this was considered to present an unacceptable risk of weld failure followed by axial movement of the components. The sun gear and planetary carriers' connection was easily solved by combining these into a one-piece part (by using shaping manufacturing techniques). The problem of how to secure the axes was solved by adding a cage to the design. Both the cage and the planetary carrier have blind (vented) holes that the axes are pressed into, without requiring any further retaining mechanism. The cage is pressed onto an axial hard stop on the planetary carrier and is then cold formed (swaged) into position. The resultant design is then both weld- and adhesive-free and enables a free choice of gear and axes materials and hardening processes.

No part involved more complexity to manufacture than the combined ring gear and motor flange for the M20 gearmotor. For industrial products, gearbox ring gears and motor flanges are usually screwed together on a large diameter thread and then either glued or welded. In the case of the M20, however, the gearmotor needs to fit inside a ring of springs, which requires a star shape pattern of wires to be precisely oriented relative to the mounting lugs on the front of the gearbox. The disadvantage of the standard assembly method is that the large diameter thread does not allow a precise angular orientation of the gearbox to the motor. The solution to this problem was to combine the flange and the ring gear into one piece. This had

the additional advantage of allowing shorter and lower mass assembly and also eliminated any unreliability in the connection. The decision required a significant reordering of the assembly sequence, but this did not cause any further problems. The manufacturing of the part itself, performed within maxon, involved a number of challenges to address, in particular the deburring of the bottom of the ring gear teeth after shaping, which required an external supplier for an electrochemical machining step and another external supplier for sand blasting the many detailed features on the motor flange.

Flight Design Issues Investigated

Detent Design

Two versions of the M32 motor were designed, with different detent strengths, each sharing components except for the magnets generating the field. The axially charged magnet in the two designs had different lengths, creating a 10 mN·m detent and a 20 mN·m detent, with the larger length baselined to enable the same housing to be used for both motor types. The step size of 24 detents per revolution was chosen to correspond to the total commutation state changes of the motor design. When paired with a gearbox, the detent size produces holding torque at a small angle at the gearmotor output.

The Hall sensors measure the edge field of the 4-pole pair continuous ring NdFeB magnet. The Hall sensors are on the output side of the motor for maxon's flat series designs, which is the same side as the detent mechanism module. When the detent was added to the motor, the performance of the detent mechanism did not match the strength of the standalone unit and motor switching error was encountered. Measurement of the magnetic field revealed the single axial magnet had significant stray flux in the vicinity of the Hall sensor, causing the switching error and reduced detent strength (Figure 5).

20mNm (with Test Motor 20-101)

- Measurement RMB influence at Hall-sensor position (Offset) without Rotormagnet:

20mNm	SSMSSSMc		SMSSSMc		SSMSSSMc	
	North outside	Bz [mT]	North outside	Bz [mT]	North outside	Bz [mT]
0.5 mm above Print	Free HS-Pos.	-1.0	Free HS-Pos.	-1.5	Free HS-Pos.	-0.5

- Offset Rotormagnet 20-101:

Test Motor 20-101	Bz [mT]	
	Offset Rotormagnet	0.2

- Measurement Hall-INL:

Test Motor 20-101	Motor only		SSMSSSMc North outside		SSMSSSMc South outside	
	CW ["el]	CCW ["el]	CW ["el]	CCW ["el]	CW ["el]	CCW ["el]
1	7.9	7.8	7.4	7.7	7.7	7.8
2	7.8	7.8	7.4	7.9	7.7	9.6
3	7.8	11.4	7.7	8.0	7.7	7.8
4	7.8	7.8	7.8	9.7	8.0	7.7
Average	7.8	8.7	7.6	8.3	7.8	8.2

Test Motor 20-101	Motor only		SSMSSSMc North outside		SSMSSSMc South outside	
	CW ["el]	CCW ["el]	CW ["el]	CCW ["el]	CW ["el]	CCW ["el]
1	7.9	7.8	10.2	9.4	6.6	5.8
2	7.8	7.8	10.6	10.5	8.3	6.0
3	7.8	11.4	9.9	9.4	6.3	6.1
4	7.8	7.8	10.0	11.0	9.7	9.0
Average	7.8	8.7	10.2	10.1	7.7	6.7

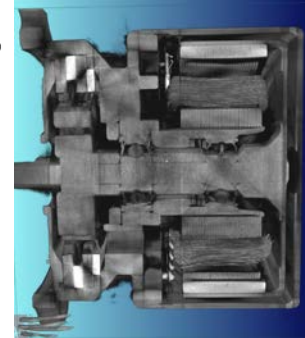


Figure 5. Left: Compensation magnet measurements for stray flux; Right: Computed Tomography (CT) scan cross section of final assembly

Two corrections were made. First, a compensation magnet axially charged in the opposite direction was added to the detent magnet stack, strengthening the field through the detent wheel. Second, the axial gap between the edge of the rotor cap ring magnet and the Hall sensor was reduced by shimming each motor individually after measuring subassembly dimensions. The change in axial gap increased the magnetic field strength and hence the signal-to-noise ratio in the Hall sensor.

Low-Quantity Grease Dosing

For the M20 gearmotor, JPL required rapid acceleration to the commanded speed without an excessive current draw over the entire specified temperature range. This is a problem due to the high viscosity of Braycote at low temperatures. The standard quantities of grease used per gearbox stage by maxon for COTS products are determined by the requirement to deliver the longest possible lifetime with standard environmental conditions. The use of Braycote required the standard quantities to be reassessed. A series of tests were performed with gearboxes built using differing quantities of grease. In each case, high frequency resolution data of the start-up current draw was collected. It was necessary to reduce the grease load by a factor of 10 compared to the standard dose in order to obtain acceptable start-up performance. Subsequent life testing demonstrated that the required life (low compared to industrial applications) could still be achieved. For the flight units, application using the grease plating method was used to ensure the low quantity of grease was uniformly distributed, a process that is unnecessary for industrial applications, where only manual dosing with a syringe at defined locations is sufficient.

The mechanism driven by the M20 actuator has a limited linear stroke. The cold drag performance of the actuator had significant transience in the first 5 seconds of motion; this large variation in torque production was outside the system-level requirements for controllability. JPL tested three actuators at several low temperatures in order to characterize the start-up current as a function of temperature. Figure 6 shows a knee in the drag happening between -30°C and -40°C for this gearbox. The actuator still exhibited margined torque production at the -70°C operation temperature limit, but due to controllability and other friction effects in the mechanism at -70°C, the heater was modified to increase the low-end operating temperature.

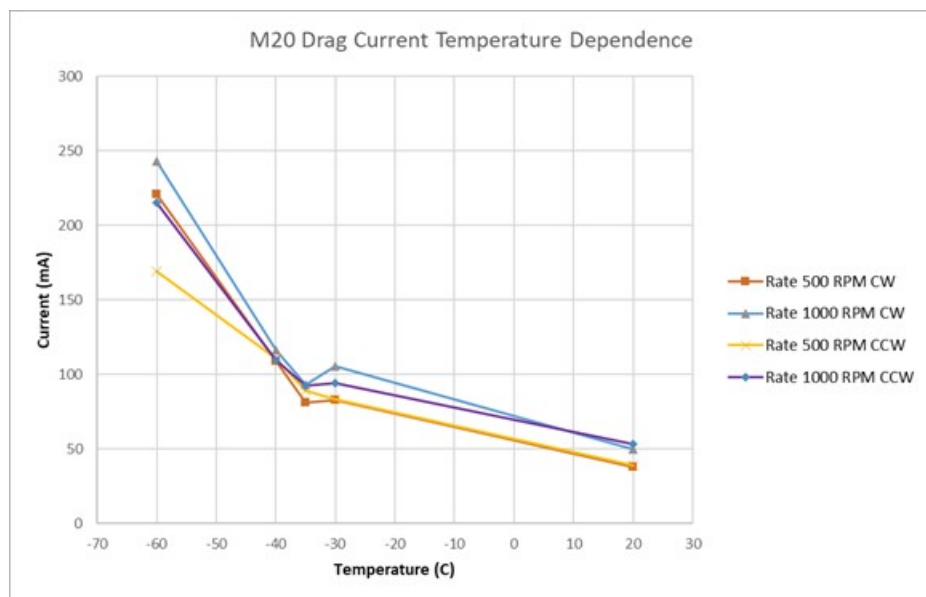


Figure 6. M20 drag current temperature dependence

Shock and Motor Bearings

The M32 motor was tested (along with the mating gearboxes) to withstand a pyroshock environment simulated by a tunable beam. The pyroshock spectrum had a peak level at 3,000-g with a knee frequency at 1,600 Hz. After testing, the motor operated with a significant rattle, a noise equated to that of a coffee grinder. Although CT scans did not reveal gross damage in the assembly, several other non-destructive tests, including a noise frequency analysis and rotating shaft deflection test, indicated motor bearings as the damaged component. The frequency analysis had peaks at the motor bearing inner ring frequency that would scale with motor speed and the deflection test had a signature reminiscent of dimples in the raceway allowing up to 0.0127 mm of deflection. The motor bearings were disassembled and inspected. The motors' front bearing inner ring, outer ring, and balls were deformed in both directions from the tunable beam test (Figure 7). The back bearing did not have any damage.

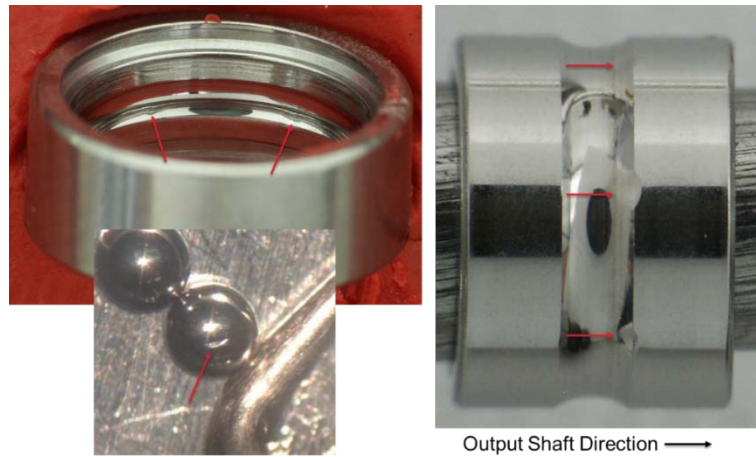


Figure 7. Damaged motor bearings from shock event

The g-level induced by pyroshock was initially analyzed with respect to the brittle components and solder/strain relief only, and did not consider the spring/mass system of the bearing/rotor combination. A design change between COTS and flight had the front bearing hard mounted in both directions, allowing the back bearing to float, resulting in the front bearing absorbing all of the energy of the accelerated rotor.

The M32 motors are used in multiple locations across the Mars 2020 rover and any changes would cause a significant project schedule impact. In most locations, the pyroshock requirement was over specified; the hardware was requalification tested to the new pyroshock requirements. The motor, and subsequent gearmotor tests, all passed the new pyroshock exposure and long rotational life requirements. There remained a single location where the motor had exposure to the high pyroshock environment but with a short rotational life. With the project considering the risk, the solution was to use the damaged motor to qualify a deployable device with high shock and limited motor rotational life. The qualification demonstrated that the damaged motor could achieve the limited revolutions needed. The flight unit was delivered and the mechanism underwent qualification at the next level of assembly. The pyrotechnic deployment was demonstrated four times and did not produce a “coffee-grinder” motor, showing that the either the requirement or tunable beam test was over conservative. In both solution cases, no changes to the flight motor were made.

Overheating Concern

The coil-to-coil resistance for the M32 and M20 motors are 14 ohms and 28 ohms, respectively. Additionally, the copper wire is wound around two PEEK stator caps at each end of the stator lamination stack, which provides thermal isolation from the bulk stator mass. The current driving the motor causes significant Joule heating due to the high resistance, quickly increasing the temperature of the low mass of copper wire insulated from the stator, which can lead to thermal runaway. The overheating worsens as the current reaches 1A.

Due to design principle requirements to demonstrate 2 \times torque at operational temperature limits, hot dynamometer tests are the highest risk activities to perform on the ground. The M32 has an additional thermal risk due to the detent mechanism; the larger holding torque design was roughly equal to the nominal performance of the motor, so twice as much current is needed during slow speeds (where the rotor has no significant inertia to carry it over the detent peaks) compared to fast speeds. A thermally instrumented unit was used to create a thermal model to understand this interaction. Guidelines for operation early on in the Mars 2020 design and qualification program were related to current input and time—a current profile could be estimated, the heat input was analyzed to confirm no overheat condition was achieved, and then a wait period was enforced in order to ensure the test article reached steady state.

The mechanism testing and subsequent system-level testing had sequences and current profiles that could not be predicted. The solution was to use a simplified thermal model on both the rover and control electrical ground support equipment (EGSE), which was the same implementation used on the MER rovers. The model is supplied with a case temperature from a platinum resistance thermometer (PRT) and the current telemetry feeds the Joule heating. The thermal protection watches for nodes and can shut down motion if temperatures rise above certain limits.

Acceptance and Qualification Testing

An acceptance test program was implemented to determine JPL acceptability of the M32 and M20 motors. The acceptance testing centered on workmanship and functional performance of each unit, whereas a qualification program subjects designated units to the gambit of JPL-margined dynamic and thermal environments and life tests to verify that the design of units from the same production and manufacturing lots would meet the mission requirements. Qualification was completed at the gearmotor level, with some actuators further qualified at the mechanism level. Portions of the M20 gearmotor qualification testing were completed at maxon using their testing facilities, where feasible. The residual tests were completed at JPL due to infrastructure availability as well as long-duration (life test) activities outside of the scope of maxon's contractual effort.

All M32 FM units were subjected to the acceptance tests listed in Table 3, with defined criteria when appropriate. No-load characterization was used as a functional check to confirm the specific motor was performing as expected and within family for the M32 flight motors.

Table 3. M32 motor acceptance tests

M32 Motor Acceptance Test	Test Conditions		Acceptance Criteria												
Dielectric strength	500V AC, 60 Hz for 60 \pm 5 seconds		I < 1 mA												
Insulation resistance (R)	500V DC, for 60 \pm 5 seconds		R > 100 M Ω												
Electrical bonding	N/A		R (flange to housing) < 25 m Ω R (flange to shaft) < 100 Ω												
Run-in	60 seconds CW and 60 seconds CCW at 28V		N/A												
Hall effect Integrated Non- Linearity (INL) sensor	Maxon defined test		<10° INL (target <7.5°)												
Natural cogging torque (T) harmonic magnitude	CW and CCW over two revolutions, speed 2 rpm		T = Detent Value (10 or 20 mN \bullet m) \pm 10%												
Powered torque ripple plot	Powered in direction of motion, powered opposite direction of motion		N/A (characterization only), validates torque is produced at all rotor positions												
Load	12V/20V/28V, CW and CCW, ambient temperature		Motor torque constant = 50 mN \bullet m/A \pm 10%												
Start-up sensitivity	CW only, 22°C /+70°C /-70°C		N/A (characterization only)												
No load	28V, CW only, 22°C /+70°C /-70°C /22°C		N/A (characterization only)												
“Launch” random vibration	<table border="1"> <thead> <tr> <th>Frequency (Hz)</th> <th>Protoflight/Design Verification (Qual/PF) Test Level</th> </tr> </thead> <tbody> <tr> <td>20</td> <td>0.15 g2/Hz</td> </tr> <tr> <td>30–90</td> <td>0.5 g2/Hz</td> </tr> <tr> <td>166–450</td> <td>0.08 g2/Hz</td> </tr> <tr> <td>2,000</td> <td>0.0040 g2/Hz</td> </tr> <tr> <td>G_{rms}</td> <td>10</td> </tr> </tbody> </table> <p>(in all 3 axes, 1 min each)</p>		Frequency (Hz)	Protoflight/Design Verification (Qual/PF) Test Level	20	0.15 g 2 /Hz	30–90	0.5 g 2 /Hz	166–450	0.08 g 2 /Hz	2,000	0.0040 g 2 /Hz	G _{rms}	10	N/A (exposure only)
Frequency (Hz)	Protoflight/Design Verification (Qual/PF) Test Level														
20	0.15 g 2 /Hz														
30–90	0.5 g 2 /Hz														
166–450	0.08 g 2 /Hz														
2,000	0.0040 g 2 /Hz														
G _{rms}	10														

Notes: CW = clockwise; CCW = counter-clockwise

The M20 motor was subjected to similar acceptance testing (Table 4) prior to integration into the M20 gearmotor.

Table 4. M20 motor acceptance tests

M20 motor Acceptance Test	Test Conditions	Acceptance Criteria
Dielectric strength	500V AC, 60Hz for 60 \pm 5 seconds	$I < 1 \text{ mA}$
Insulation resistance	500V DC, for 60 \pm 5 seconds	$R > 100 \text{ M}\Omega$
Electrical bonding	N/A	$R \text{ (flange to housing)} < 25 \text{ m}\Omega; R \text{ (flange to shaft)} < 100 \text{ }\Omega$
Run-in	60 sec CW and 60 sec CCW at 28V	N/A
Hall effect (INL) sensor	Maxon defined test	$<10^\circ \text{ INL}$
Torque ripple	CW and CCW over one revolution	N/A (characterization only), validates torque is produced at all rotor positions
No load	24V, CW and CCW, 22°C	N/A (characterization only)

The acceptance tests listed in Table 5 were completed at the M20 gearmotor level, which included thermal environment exposure at non-operational temperature limits of -135°C.

Table 5. M20 gearmotor acceptance tests

M20 Gearmotor Acceptance Test	Test Conditions			Acceptance Criteria	
Run-in	7.5 minutes CW and 7.5 minutes CCW at 24V			N/A	
Back drive torque	Ramp to 75 mN•m, CW only			Static holding torque: $> 50 \text{ mN}\cdot\text{m}$	
No load	24V, CW only, STP			N/A (characterization only)	
"Launch" random vibration	Frequency (Hz)	Protoflight/Design Verification (Qual/PF)	Test Level	N/A (exposure only)	
	20	0.15 g ² /Hz			
	30–90	0.5 g ² /Hz			
	166–450	0.08 g ² /Hz			
	2,000	0.0040 g ² /Hz			
	G _{rms}	10			
(in all 3 axes, 1 min each)					
Non-operational thermal	One thermal cycle from +113°C to -135°C Two thermal cycles from +70°C to -135°C			Restrain static holding torque ($T > 50 \text{ mN}\cdot\text{m}$)	
Operational thermal	Each test performed at +70°C/22°C/-70°C			Gearmotor torque constant = 1620 N•m/A \pm 10%	
Start-up sensitivity	CW only				
No load	24V, CW only				
Load	12V/20V/28V, CW and CCW				

The majority of the M32 and M20 hardware subjected to acceptance testing met performance requirements and were accepted as meeting flight fidelity.

JPL accepted the risk of qualifying the M20 actuator post delivery of the flight units due to the schedule criticality of needing the flight hardware assembly. Tests completed by JPL to fully qualify the design (Table 6) exposed an actuator to the flight acceptance test (with the exception of 2 minutes per axis random vibration exposure) and then completed a long-duration thermal bakeout, pyroshock, and humidity exposure. The gearmotors underwent a long-duration thermal vacuum bakeout to replicate the maximum expected exposure the assembled mechanisms may be subjected to in order to meet Planetary Protection requirements. The gearmotors were also subjected to 40 hours of accelerated corrosion exposure in an 80°C/80% relative humidity environment meant to simulate any corrosion that may occur in the gearbox while exposed to the Earth's atmosphere before launch. The gearmotor was then subject to the rotary life test. A separate motor-only unit was subjected to the thermal life test.

The rotary life qualification unit completed its life test with minimal wear, and the design completed qualification for flight as of June 2018. The Thermal Life test is 1.5 years in duration and was successfully completed in December 2019.

Table 6. M20 gearmotor qualification tests.

M20 Gearmotor Qualification Test	Test Conditions		Acceptance Criteria								
Thermal vacuum bake-out	113°C ±2°C at 1.3×10^{-3} Pa for 288 hours		N/A (exposure only)								
Pyroshock	Tunable beam (2 hits in 2 axes) <table border="1" style="margin-top: 10px;"> <thead> <tr> <th>Frequency (Hz)</th> <th>Shock Response Spectrum (SRS) Level (Q = 10)</th> </tr> </thead> <tbody> <tr> <td>100</td> <td>5 g</td> </tr> <tr> <td>100–3,500</td> <td>+9.0 dB/Oct.</td> </tr> <tr> <td>3,500–10,000</td> <td>1,000 g</td> </tr> </tbody> </table>		Frequency (Hz)	Shock Response Spectrum (SRS) Level (Q = 10)	100	5 g	100–3,500	+9.0 dB/Oct.	3,500–10,000	1,000 g	N/A (exposure only), in family with no-load characterization
Frequency (Hz)	Shock Response Spectrum (SRS) Level (Q = 10)										
100	5 g										
100–3,500	+9.0 dB/Oct.										
3,500–10,000	1,000 g										
Humidity exposure	40 hours of 80% humidity/+80°C		N/A (exposure only)								
Rotary life test	Torque bins: 0.2 N•m for 40,400 revolutions 0.3 N•m for 12,400 revolutions 0.4 N•m for 2,100 revolutions 0.5 N•m for 1,500 revolutions Split between CW and CCW and alternating between +70°C, +22°C, -55°C, and -70°C		In family with no-load characterization								
Thermal life test	3015 thermal cycles (4.5 Mars years) broken into seasonal profiles (-80°C to +85°C for summer and -115°C to +50°C for winter)		In family with no-load characterization at interval checks								

Final Delivery

For the nine flight locations of the M32 motor across the Mars 2020 rover, a total of 37 gearmotors were needed to meet flight, flight spare, engineering model (EM), and qualification units. maxon required a minimal build to efficiently use their production and manufacturing series, which resulted in three lot builds (EM1, FM1, FM2) totaling 99 delivered M32 units. The 99 units consisted of 10 EM1s (3× 10 mN•m and 7× 20 mN•m), 35 FM1s (14× 10 mN•m and 24× 20 mN•m), and 54 FM2s (33× 10 mNm and 21× 20 mNm). Similarly, the M20 gearmotor had a JPL need of 6 units but a total of 40 units were delivered. The 40 units consisted of 16 EMs and 24 FMs. On the FM units, the carriers with sun gear were made out of two different material types, with 12 units of each type delivered. An attrition of over 50% during the manufacturing and production phases had delivery effects but the flexibility and availability of the on-site facilities allowed maxon to recoup schedule as best as possible and phase deliveries between the lots as needed.

Due to the surplus of flight units available, JPL was able to cherry-pick motors with the optimum performance and flight fidelity for the 10 flight units. The residual units are logged in the JPL flight hardware logistics program for future NASA project use. Additionally, maxon has a catalog flight-qualified specification for the M32 and M20 flat motors.

Conclusions and Lessons Learned

Detent Design

Although the detent brake worked well and the add-on module that was designed proved capable of passing all qualification tests, this solution adds mass and complexity. In parallel, work was carried out by maxon to make rotors with segmented magnets (rather than a one-piece ring magnet) and then shape the magnetic field from those magnets to create the necessary detent. Making magnetic field simulations that correctly predicted the obtained detent was difficult, which resulted in initial prototypes delivering insufficient torque. Follow-up prototypes achieved the targeted 10 mNm. The greatest difficulty encountered was fixing the individual magnets to the rotor so that they were not susceptible to breaking under shock impacts. Eventually it was decided that this presented too much risk, especially to the schedule if several attempts were needed to find a workable solution. Despite not being chosen for the flight design, with further development this is likely to be a more reliable (because of fewer parts) and compact solution that should be investigated further.

Overheating Concern

The overheating concern has led to significant efforts in both analysis and implementation to reduce the motor wire temperature below the allowable limits. For past missions, protecting the motors from overheating entailed installing a PRT on the case and operating under the assumption that the housing temperature is well coupled to the wire temperature. Due to the outer rotating design of the Mars 2020 motors, there is no external location that is thermally coupled. However, a potential solution for both ground testing and thermal model validation would be to implement a thermocouple (TC) directly into the windings at the time of assembly and provide a path for those thermocouples to be monitored, either through traces in the board or holes in the board that can be routed to the channel for the lead wires. These thermocouples can be set to a GSE thermal alarm or act like a switch. The TCs can monitor concurrently while running the thermal model in multiple atmospheric environments to better ground the model in demonstrated performance. An additional improvement to the design could be to thermally couple the wires to the stator lamination stack instead of suspended between two PEEK end caps.

Teamwork between a Government-Funded Science Institution and a Commercial Company

A close collaboration between maxon and JPL was essential in developing the flight units, as it required a combination of maxon's decades of experience with industrial motor and gearbox design and JPL's decades of institutional experience in spacecraft design.

For such a collaboration to work, it is necessary for both sides to understand each other's motivations and methodologies. Commercial companies (especially those with limited previous space experience) need to understand that organizations like JPL can (and do) place significant resources into issues that may be of no importance in an industrial setting, which is a result of decades of hard learnt lessons where a single small failure can terminate a mission. The space environment is very unforgiving of design or manufacturing errors, which may never be noticed in a standard Earth-based application. The education of contractor staff on this history is a critical part of gaining acceptance for the space science mission method of working.

In turn, government-funded institutions need to understand how industrial manufacturing companies, such as maxon, usually have the goal of using their limited engineering resources as efficiently as possible to keep the production lines filled with products that receive repeat orders. Thus, one-off high engineering resource developments are often viewed as a disturbance to the series production goals of the company; however, this can be partially mitigated by presenting the work as subsidized technology development and being as open as possible in helping the commercial company obtain a marketing effect by publicizing the work.

Final Thoughts

During the three-year collaboration, significant resources were required from both organizations to resolve the problems encountered and complexity involved in developing the Mars 2020 actuators. Even when the basis of the design was a commercial product, the issues encountered highlight the importance of allowing

sufficient time in mission planning for solution development. It was pivotal for JPL and maxon to leverage experts at each location to address critical problems (along with using a 9-hour time difference between Luzern and Los Angeles to accomplish an 18-hour project work day).

Both the M20 and M32 designs have been successfully qualified. The M32 designs were integrated into three different, separately sourced gearboxes and passed all qualification testing. The two versions of the M32 motor are implemented into nine locations on the Mars 2020 rover and the M20 is integrated into a single location. Flight model hardware has been built, acceptance tested, integrated into the target gearboxes and mechanisms, and installed on the Mars 2020 rover awaiting launch to Mars in July 2020 (Figure 8).

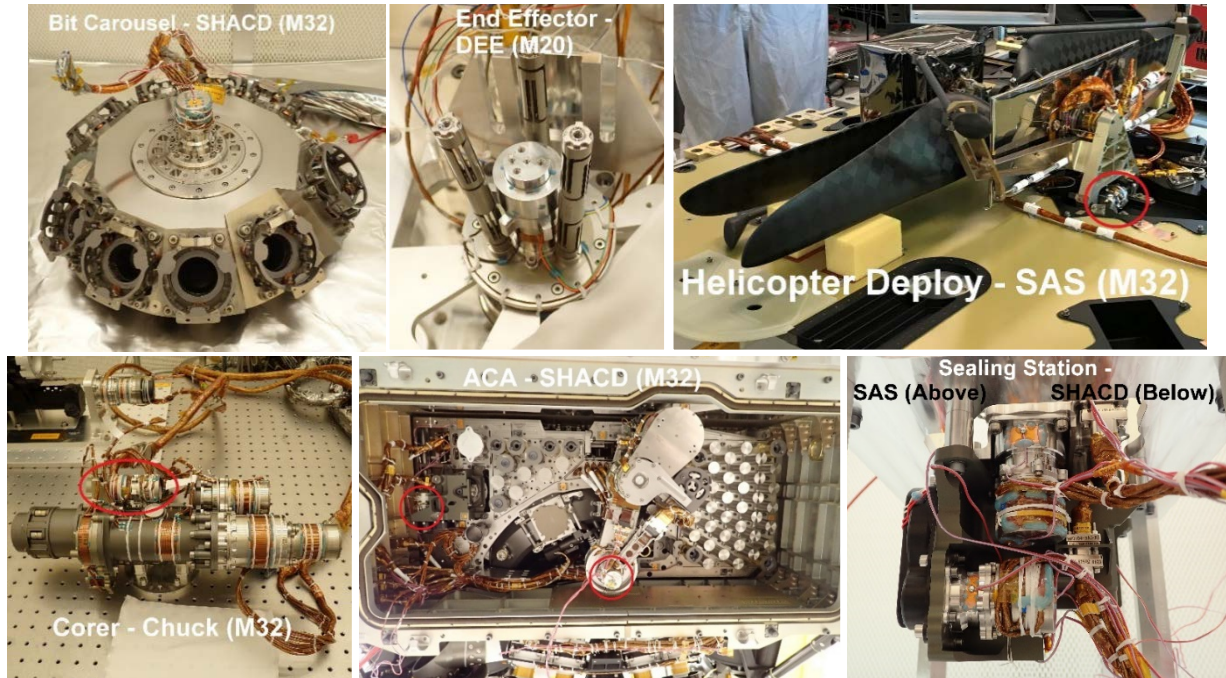


Figure 8. maxon hardware installed on Mars 2020

Acknowledgements

The successful collaboration and delivery of the maxon flight motors to Mars 2020 would not be possible without many individuals at JPL and maxon over the three-year effort. In addition, the authors would like to thank their families who endured years of middle-of-the-night teleconferences and nights away on international trips.

The research was carried out at the Jet Propulsion Laboratory, California Institute of Technology, under a contract with the National Aeronautics and Space Administration.

References

1. NASA Procedural Requirements, NPR 8705.4 (2004),
https://nодis3.gsfc.nasa.gov/npg_img/N_PR_8705_0004 /N_PR_8705_0004 .pdf.
2. Braun, David and Don Noon, "Long Life" DC brush motor for use on the Mars Surveyor Program, 32nd *Aerospace Mechanisms Symposium* (1998).
3. See graphic on page 2 of Ref. [5], or this direct link: <https://mars.nasa.gov/imgs/2013/07/mars-exploration-timeline-07-2016-hpfeat2.png>.
4. Office of Inspector General, NASA's Mars 2020 Project, Report no. IG-17-009 (2017),
<https://oig.nasa.gov/docs/IG-17-009.pdf>.
5. NASA, Mars 2020 Mission Overview, available at: <https://mars.nasa.gov/mars2020/mission/overview/>.
6. Szwarc, Timothy, Jonathan Parker, and Johannes Kreuser, STIG: A Two-Speed Transmission Aboard the Mars 2020 Coring Drill, 45th *Aerospace Mechanisms Symposium* (2020).
7. Chrystal, Kyle, Percussion Mechanism for the Mars 2020 Coring Drill, 45th *Aerospace Mechanisms Symposium* (2020).
8. Barletta, Anthony, Design and Development of a Robust Chuck Mechanism for the Mars 2020 Coring Drill, 45th *Aerospace Mechanisms Symposium* (2020).
9. Silverman, Milo and Justin Lin, Mars 2020 Rover Adaptive Caching Assembly: So Many Challenges, 45th *Aerospace Mechanisms Symposium* (2020).
10. Grimes-York, Jesse and Ken Glazebrook, Sealing Station Mechanisms for the Mars 2020 Rover Sample Caching Subsystem, 45th *Aerospace Mechanisms Symposium* (2020).
11. Brown, Adrian, Mars Science Laboratory: the technical reasons behind its delay, *The Space Science Review* (2009), <http://www.thespacereview.com/article/1319/1>.
12. Phillips, Robin R., M. Palladino, and C. Courtois, Development of Brushed and Brushless DC Motors for use in the ExoMars Drilling and Sampling Mechanism, *Aerospace Mechanisms Symposium* (2012).
13. McCoubrey, R., et al., Canada's Suspension and Locomotion Subsystem for ExoMars 2018, 65th *International Astronautical Congress*, Toronto, Canada (2014).
14. Herman, Jason and Kiel Davis, Evaluation of Perflouropolyether Lubricant Lifetime in the High Stress and High Stress-Cycle Regime for Mars Applications, 39th *Aerospace Mechanisms Symposium* (2008).

